Cancer Management and Research

Dovepress

open access to scientific and medical research

Open Access Full Text Article

ORIGINAL RESEARCH

Multiphoton microscopy in the diagnostic assessment of pediatric solid tissue in comparison to conventional histopathology: results of the first international online interobserver trial

This article was published in the following Dove Press journal:
Cancer Management and Research

Jan Goedeke[1]
Peter Schreiber[1]
Larissa Seidmann[2]
Geling Li[3]
Jérôme Birkenstock[4]
Frank Simon[1]
Jochem König[5]
Oliver J Muensterer[1]

[1]Department of Pediatric Surgery, University Medical Center of the Johannes Gutenberg-University Mainz, 55131 Mainz, Germany; [2]Institute for Pathology, University Medical Center of the Johannes Gutenberg-University Mainz, 55131 Mainz, Germany; [3]Department of Pediatric Pathology, Childrens Hospital of Alabama, University of Alabama at Birmingham, Birmingham, AL 35233, USA; [4]Forschungszentrum für Translationale Neurowissenschaften, University Medical Center of the Johannes Gutenberg-University Mainz, 55131 Mainz, Germany; [5]Institute of Medical Biostatistics, Epidemiology and Informatics (IMBEI), University Medical Center of the Johannes Gutenberg-University Mainz, 55131 Mainz, Germany

Purpose: Clear resection margins are paramount for good outcome in children undergoing solid tumor resections. Multiphoton microscopy (MPM) can provide high-resolution, real-time, intraoperative microscopic images of tumor tissue.

Objective: This prospective international multicenter study evaluates the diagnostic accuracy, feasibility, and interobserver congruence of MPM in diagnosing solid pediatric tissue and tumors for the first time.

Material and methods: Representative fresh sections from six different neonatal solid tissues (liver, lung, kidney, adrenal gland, heart muscle, testicle) and two types of typical pediatric solid tumors (neuroblastoma, rhabdomyosarcoma) with adjacent nonneoplastic tissue were imaged with MPM and then presented online with corresponding H&E stained slides of the exact same tissue region. Both image sets of each tissue type were interpreted by 38 randomly selected international attending pediatric pathologists via an online evaluation software.

Results: The quality of MPM was sufficient to make the diagnosis of all normal tissue types except cardiac muscle in >94% of assessors with high interobserver congruence and 95% sensitivity. Heart muscle was interpreted as skeletal muscle in 55% of cases. Based on MPM imaging, participating pathologists diagnosed the presented pediatric neoplasms with 100% specificity, although the sensitivity reached only about 50%.

Conclusion: Even without prior training, pathologists are able to diagnose normal pediatric tissues with valuable accuracy using MPM. While current MPM imaging protocols are not yet sensitive enough to reliably rule out neuroblastoma or rhabdomyosarcoma, they seem to be specific and therefore useful to confirm a diagnosis intraoperatively. We are confident that improved algorithms, specific training, and more experience with the method will make MPM a valuable future alternative to frozen section analysis.

Registration: The trial was registered at www.researchregistry.com, registration number 2967.

Keywords: multiphoton microscopy, pediatric tissue, solid tumors, pediatric, conventional histopathology, interobserver trial

Correspondence: Jan Goedeke
Department of Pediatric Surgery, University Medical Center of the Johannes Gutenberg-University Mainz, Langenbeckstr. 1, 55131 Mainz, Germany
Tel +49 613 117 2034
Fax +49 613 117 6523
Email jan.goedeke@unimedizin-mainz.de

Introduction

Exact histopathologic diagnosis is a cornerstone in the successful treatment of different pediatric solid tumors, for which complete local control within an uncompromised resection margin dramatically decreases the risk of recurrence and increases survival. In other indications, such as Hirschsprung's disease, exact,

submit your manuscript | www.dovepress.com
DovePress
http://doi.org/10.2147/CMAR.S195470

intraoperative histopathologic diagnosis is mandatory for the exact determination of the transition zone and the possible resection margins as well. Although still considered the intraoperative gold standard with overall sensitivity up to 89% in establishing diagnosis, frozen section histopathology (HP) requires time-consuming tissue processing and can sometimes require repeat biopsies if the initial specimen is nondiagnostic.[1–3]

Intraoperative frozen section also means working under considerable temporal and procedural stress for many pathologists, because during frozen section analysis, it is hardly possible to resort to supplementary diagnostic methods such as immunohistochemical stainings, which are standard for some diseases in addition to conventional HP and sometimes necessary for proving the diagnosis. To overcome some of the obstacles associated with histopathologic processing, efforts have been made to develop high-resolution live imaging techniques, and in particular, multiphoton microscopy (MPM). In principle, this technique allows real-time visualization of suspicious lesions at cellular and subcellular levels, followed by the intraoperative resection of only the pathologic lesions, thereby reducing sampling error and minimizing patient morbidity associated with unnecessary excisional biopsies. Different published studies of Jain et al already tested MPM as a potential "optical biopsy" tool for real-time evaluation of lung tumors without the need for exogenous contrast agents, and for determination of carcinoma in situ in human bladder or the extended evaluation and differentiation of renal carcinoma.[4–7]

Likewise, MPM could also help to reduce intraoperative trauma and improve patient´s potential outcome by intraoperatively identifying and sparing neural tissue.[8]

So far, MPM has not been studied for childhood tumors or other pediatric indications. Partially, this is due to the lack of clinically compatible MPM devices, outside the realms of dermatology or animal experiments.[9–11]

There is also a lack of reference data for MPM image interpretation, especially for children. In our previous proof-of-principle pilot study, we therefore described for the first time the use of MPM as a promising, new tool for the additional evaluation of solid pediatric tumors.[12]

The primary objective of the present study was to go one step further and to evaluate the diagnostic accuracy, feasibility, and interobserver congruence of MPM versus conventional histopathology (as gold standard) for normal pediatric tissues and two typical pediatric solid tumors by attending pediatric pathologists. Because of the lack of adequate reference data, we were only able to rely on the promising data of our pilot study. Our main hypotheses were that MPM is as accurate as conventional pathology for selected issues of pediatric solid tissue in interpretation by MPM-naive but otherwise experienced board-certified pediatric pathologists or other pathologists who interpret pediatric tissue at their center.

Normal tissues were selected to describe how different tissue characteristics are visualized by MPM to allow the identification of potentials and pitfalls. Neuroblastoma and rhabdomyosarcoma were selected as entities for this study because we feel they are the most likely tumors requiring timely and accurate intraoperative diagnosis, in which MPM may be helpful.

Material and methods

Study design

This study was designed as an international multicenter trial, in which specialized pediatric pathologists or pathologists that interpret pediatric tissues at their center were asked to interpret a variety of different normal and neoplastic tissues via an Internet online survey. The responses were used to evaluate the accuracy, feasibility, and interobserver congruence of MPM in diagnosing representative solid pediatric tissue and tumors in comparison to the gold standard method (conventional HP, H&E staining). The study was performed in compliance with the STARD 2015 Guidelines for reporting diagnostic accuracy studies.[13,14]

The trial was registered at www.researchregistry.com, registration number 2967. The full study protocol in detail is available on this platform. Ethics board approval was granted by the physician board of the state of Rhineland-Palatinate, number 837.274.15 (10,042). Both written and informed consent were obtained from all parents or guardians included in the study. All procedures performed in studies involving human participants were in accordance with the ethical standards of the institutional and/or national research committee and with the 1964 Helsinki declaration and its later amendments or comparable ethical standards. The study actual online evaluation was conducted prospectively from November 2017 to December 2017.

Study cohort and recruitment

International board-certified attending pathologists dealing with pediatric tissues were randomly recruited via an online search to participate in this study. The basic requirement was the special qualification in pediatric pathology and

inexperience with MPM for childhood tissue evaluation. Participation was voluntary and was not remunerated. There was no intended sample size, as no reference data were available yet, and therefore, a pre-hoc power analysis was not possible.

Specimen acquisition

We acquired formalin fixed and paraffin embedded normal neonatal tissues (liver, lung, heart, kidney, adrenal gland, testicle) from the ethics-board approved pediatric tissue bank of our institutional pathology unit and freshly removed, formalin fixed and paraffin embedded tumor tissue (neuroblastoma, rhabdomyosarcoma) to obtain MPM and conventional HP images incorporated into the online survey. Informed consent to participate in the study was obtained from the parents of the children who underwent tumor resection.

MPM imaging

Specimen handling

For the direct comparison of MPM with conventional HP, an average of 16 slides was prepared from selected and representing native tissue blocks. All slices were cut with a microtome to a thickness of 3 µm to facilitate imaging of the same structures by both methods. The HP slides were processed with conventional H&E staining, the MPM slides remained unstained.

Specimen imaging

Imaging was performed as previously described in our prior publication.[12]

We used a two-photon laser-scanning microscope (Leica TCS MP5; Leica Microsystems, Wetzlar, Germany). Figure 1 shows a schematic setup of the microscope. The acquired images were exported as TIFF-files and for superimposing (post-processing) the image channels (red, green) and for brightness adjustment Photoshop software (Adobe Systems Software Ltd., Dublin, Ireland) was used. The tissues were excited using a tunable femtosecond pulsed titansaphire-laser at 950 nm (Chameleon Ultra, Coherent Inc., Santa Clara, CA, USA), controlled by Leica LAS-AF Software (Leica Application Suite, Leica Microsystems, Wetzlar, Germany). Images were obtained through a Leica HCX IRAPO L 25×/0,95 W objective and a BS 505 beam splitter. Two separate filters were used (CFP BP 483/32 nm [cyan], YFP BP 535/30 nm [yellow]).

The CFP BP 483 signal captures autofluorescence of the tissue and was false color-coded in green, while the YFP BP 535 signal represents second harmonic generation and was color-coded in red. Hence, intracellular components are featured in green, while collagen, actin, myosin and tubulin are depicted in red on the final post-processing MPM images.

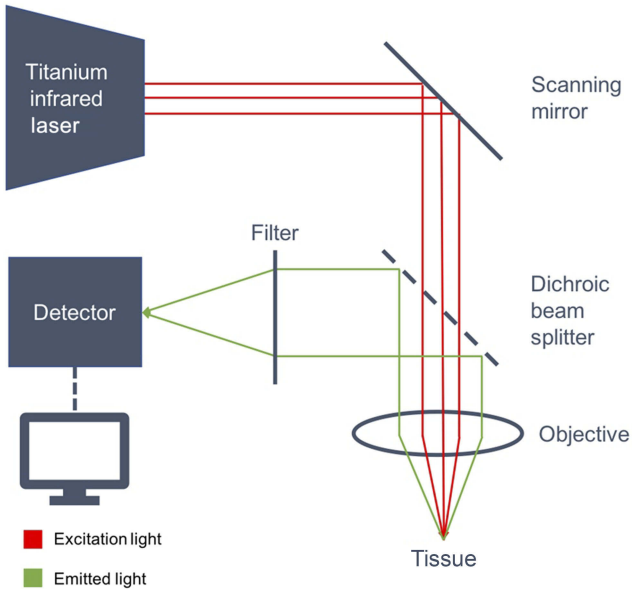

Figure 1 Schematic setup of the multiphoton microscope. Focal tissue is excited using pulsed laser light (red arrows). The resulting signal is processed through an objective/splitter/filter system and captured by a detector to create the image.

Field of view was set at 620 µm×620 µm. Higher scanner zoom was used when necessary. In order to increase the penetration depth within the tissue, the detection unit was placed in immediate vicinity of the sample. Z-stacks of multiple images were produced by collecting a series of images moving from the tissue surface toward deeper layers.

Slide sample selection for online survey

Several samples of conventional HP slides and corresponding MPM images of all tissues were collected and valued in advance in collaboration with the local pediatric pathology attending. For the online survey, one pair of each tissue was randomly selected.

Interobserver online survey and data collection

To assess the diagnostic potential of MPM, an international online survey was conducted. For this purpose we used QuestionPro© survey software (QuestionPro©, 548 Market St # 62790 San Francisco, CA 94104-5401), which

was made available through a university license. All data were gathered prospectively.

The participating pathologists were asked to click a system-generated URL link that was available worldwide via the Internet. The participant ratings were collected anonymously.

All images were uploaded by the study team as high-resolution TIFF files in QuestionPro© and could be zoomed in by the participants up to twice the size. Participants were blinded to all patient information, including the final histopathologic diagnosis, to answer the first two questions.

In the first step of each test, the assessment of an MPM image and the definition of the general tissue type were based on six given options in multiple-choice format. This was intended to determine the primary identifiability on the MPM image regarding the tissue type (primary outcome parameter). There was no time limit in the assessment and only a single answer could be given.

Subsequently, the participant was redirected to a second, independent page of the survey, without the possibility to return to the previous (first) page. Here, a conventional H&E stained HP slide from the same cutting plane as the MPM image before was presented, and the participant was asked to identify the tissue type again.

In the third step, the participant was redirected to another questionnaire and asked to directly compare the MPM image and the conventional HP image after official announcement of the actual correct tissue type. Participants were asked to grade the clarity of specific histologic features (such as cell nucleus, collagen fibers, etc.) as the tertiary outcome parameter.

Typical features of each specific tissue were established beforehand and presence of these features was either confirmed or refuted on MPM and the corresponding conventional HP images in a simple grading system (0 [not visible], 1 [suggested without details], 2 [recognizable without further details], 3 [recognizable including all details]).

The overall process was repeated for the six normal neonatal tissues (liver, lung, heart muscle, kidney, adrenal gland and testicle) and the two solid childhood tumors (adrenal gland neuroblastoma and bladder embryonal rhabdomyosarcoma).

Since all of the tissues in our study were, to our best knowledge, never evaluated by MPM before, no published reference data were available. The full survey can be accessed at https://www.questionpro.com/t/ANSLnZbAvU.

Selective connective tissue/cell nuclei assessment

Following the online survey, we individually assessed the scoring of connective tissue-containing structures and cell nuclei across all tissue samples on the basis of the study results.

Statistical analysis

All statistical analyses were performed using SPSS (version 23, IBM, NY, USA).

The primary and secondary outcome parameters were compared and described as means and 95% CIs. In the following step, MPM diagnosis was compared with H&E diagnosis using McNemar's test for two paired binary random variables. An alfa error of $P<0.05$ was considered statistically significant. A standard 2×2 contingency table was used to determine the diagnostic overall test operating characteristics (sensitivity, specificity, positive predictive value and negative predictive value).

The tertiary outcome parameters were described as means and 95% CIs. Values were compared using the paired samples Wilcoxon test. For detailed analysis of cell nuclei and connective tissue structures, values were compiled descriptively across all organs and tumors, and also compared using the Wilcoxon ranking test.

To examine the strength of the inter-rater reliability (IRR), Randolph's free-marginal multi-rater *kappa* was used to evaluate the validity of the survey.[15]

Results

Study participants

One hundred ninety-eight international pathologists with specialization in pediatric pathology were randomly invited for study participation. Addresses were found by an Internet search for "pediatric pathologist" and online information published on international national pathology associations. The response rate was 21.2% (n=42). In total, 38 participants from 13 different countries were defined as eligible for study participation and all participants completed the survey. Participants were enrolled between November 2017 and December 2017. An overview of the distribution of participants is shown in Figure 2. All study participants answered the questions completely and no data are missing. The average survey time for each participant was 25.35 mins (95% CI: [19.75, 30.95]) for 32 questions.

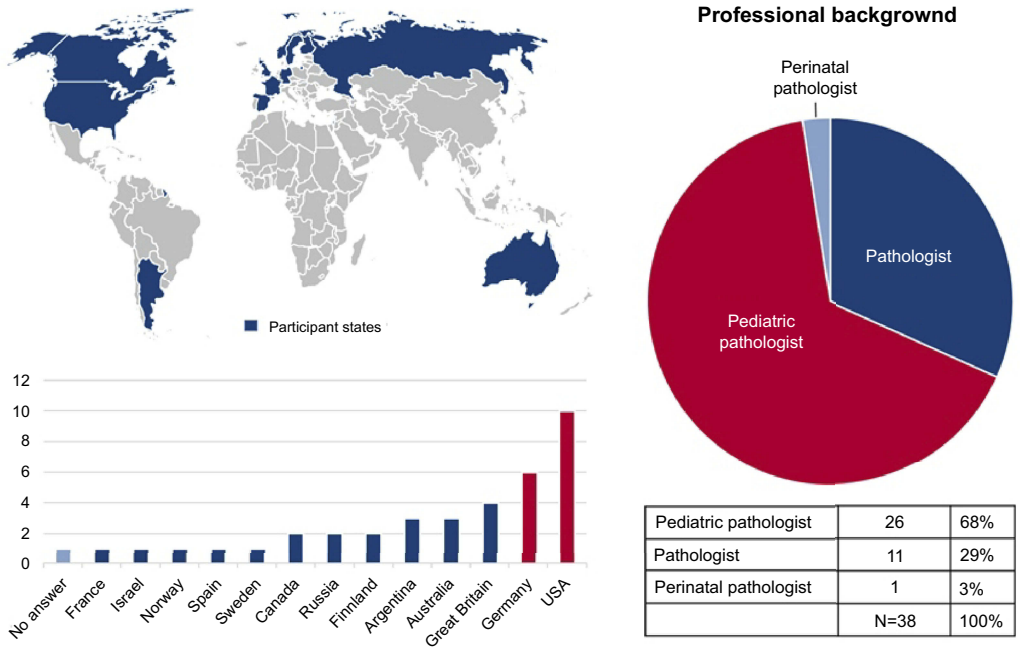

Pediatric pathologist	26	68%
Pathologist	11	29%
Perinatal pathologist	1	3%
	N=38	100%

Figure 2 Overview of the origin of the participants.

Primary outcome parameter – detectability on MPM

Recognition of tissues based on initial MPM image only

The normal tissues were identified correctly on MPM in >94% without knowing the image in advance (see Table 1). For the representative image of the lung, the adrenal gland and the testicle, the sensitivity reached 100%. Overall, only the heart muscle was incorrectly identified frequently (44.7%) and often interpreted as skeletal muscle instead. Only 34.2% of the participants identified the tumor entity of the neuroblastoma and only 47.4% of the tumor entity of the rhabdomyosarcoma on MPM initially. In total, 5.37 (95% CI: [5.16, 5.58]) of 6 healthy solid neonatal tissues were identified correctly per participant. Together with the tumor tissues, a primary detectability of 6.18 (95% CI: [5.82, 6.55]) of a total of 8 tissues was found.

Comparative MPM and H&E stained images of benign testicular tissue and a bladder rhabdomyosarcoma are shown as an example in Figure 3.

Secondary outcome parameter – detectability on H&E stains

Recognition of the tissue entity based on the conventional H&E stained image and comparison with MPM

The H&E stained image was rated correctly in >92% in 5 of 6 solid neonatal tissues without knowing the correct answer in advance (see Table 1), but having seen the MPM image of the respective tissue before. For the representative image of liver and adrenal gland, the sensitivity reached 100%. Only heart muscle has low identification rates (71.1%). Overall, 73.7% of the participants identified the tumor entity of the neuroblastoma, and 81.6% the tumor entity of the rhabdomyosarcoma correctly after seeing both the MPM and H&E images.

In total, 5.66 (95% CI: [5.48, 5.83]) of 6 healthy solid neonatal tissues were identified correctly per participant on H&E conventional histopathology. Together with the tumor tissues, a primary detectability of 7.21 (95% CI: [6.90, 7.52]) of a total of 8 tissues was found.

The comparison of both imaging techniques revealed no significant differences for correct characterization of the healthy neonatal liver, lung, kidney, adrenal gland and testicle. Heart tissues and both tumors were recognized more often on H&E conventional HP compared to MPM.

Regarding the contingency table comparing MPM with final histopathologic diagnosis as the gold standard for normal solid pediatric tissue and tumor tissue separately see Table 2.

Tertiary outcome parameters

Evaluation of specific parameters of the individual tissues

The recognizability of specific tissue characteristics is presented in Table 3.

In the assessment of the specific tissue characteristics of the tumors entities, conventional HP was significantly better

Table 1 Descriptive tissue entity evaluation of MPM versus conventional HP (H&E). Significantly better rating marked in bold and italics

	MPM	H&E	*P*
Participants n	38	38	n.s.
Primary assessment of tissue entity	Correct answers (sensitivity; % of total)	Correct answers (sensitivity; % of total)	
Liver	37/38 (97.4%)	38/38 (100%)	n.s.
Lung	38/38 (100%)	35/38 (92.1%)	n.s.
Heart	17/38 (44.7%)	**27/38 (71.1%)**	0.002
Kidney	36/38 (94.7%)	37/38 (97.4%)	n.s
Adrenal gland	38/38 (100%)	38/38 (100%)	n.s
Testicle	38/38 (100%)	37/38 (97.4%)	n.s
Neuroblastoma	13/38 (34.2%)	**28/38 (73.7%)**	<0.001
Rhabdomyosarcoma	18/38 (47.4%)	**31/38 (81.6%)**	<0.001

Note: Bold values indicate H&E was statistically significantly superior to MPM for the evaluation of heart, neuroblastoma and rhabdomyosarcoma tissue.
Abbreviations: MPM, multiphoton microscopy; H&E, hematoxylin-eosin; n.s., nonsignificant; HP, histopathology.

rated compared to the MPM. Only the stromal assessment with tumor vessels in neuroblastoma was equivalent (see Table 3).

Selective assessment of cell nuclei

The assessment of cell nuclei was rated significantly lower ($p<0.001$) on MPM images (normal tissue and tumors) compared to conventional HP (see Table 4).

Selective evaluation of connective tissue structures

The assessment of almost all connective tissue-containing structures was rated significantly lower ($p<0.001$) on MPM images (normal tissue and tumors) compared to conventional HP (see Table 4). MPM was equivalent to conventional HP in the testicular evaluation except for cell nuclei. Identification of the septum testis was rated significantly better on MPM images, as was the identification of the disci intercalares in heart musculature. An overview about the considered structures is shown in Table 5.

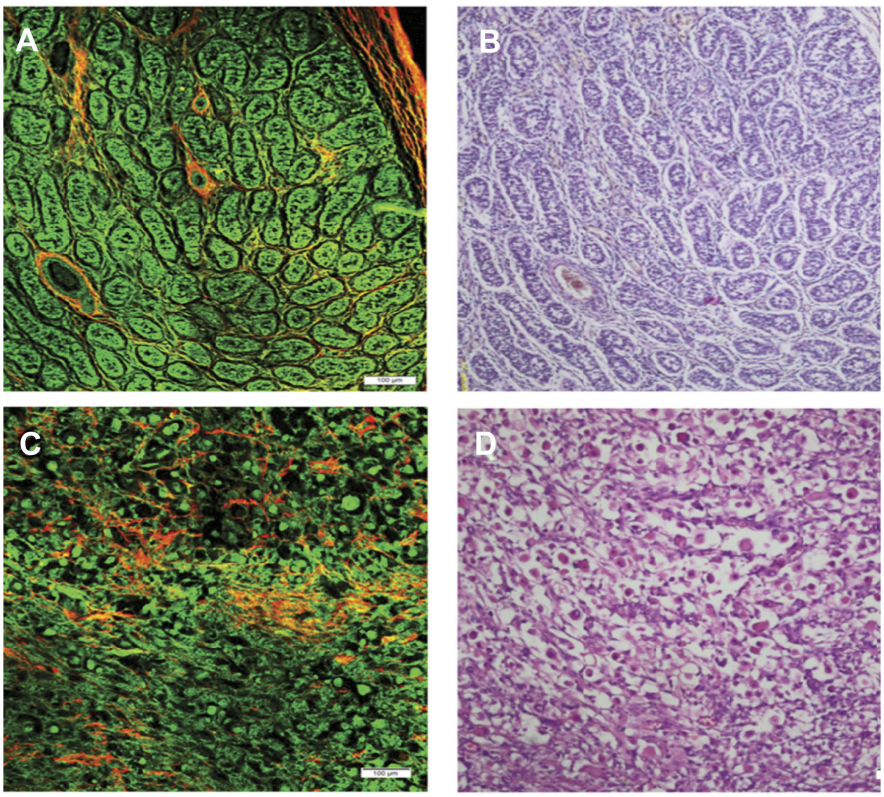

Figure 3 Comparative MPM and H&E stained images of benign testicular tissue (**A** and **B**) and rhabdomyosarcoma (**C** and **D**). Collagen fibers appear color-coded red on MPM, Tubuli seminiferi contorti (testis) and nuclei of rhabdomyoblasts and parts of myxoid stroma (rhabdomyosarcoma) appear green.
Abbreviations: MPM, multiphoton microscopy; H&E, hematoxylin-eosin; n.s., nonsignificant; HP, histopathology.

Table 2 A 2×2 contingency table comparing tissue identification of MPM with conventional HP

			H&E diagnosis						H&E diagnosis					
			Correct	Incorrect					Correct	Incorrect			Correct	Incorrect	
MPM diagnosis	Correct	204	0	PPV=95% NPV=100%	MPM diagnosis	Correct	18	0	PPV=58% NPV=100%	MPM diagnosis	Correct	13	0	PPV=46% NPV=100%
	Incorrect	11	13			Incorrect	13	7			Incorrect	15	10	
		Sensitivity=100%	Specificity=54%				Sensitivity=100%	Specificity=35%				Sensitivity=100%	Specificity=40%	
Healthy tissue					**Rhabdomyosarcoma**					**Neuroblastoma**				

Abbreviations: MPM, multiphoton microscopy; NPV, negative predictive value; PPV, positive predictive value.

Evaluation of interobserver agreement

The overall IRR calculated with Randolph's free-marginal multi-rater kappa was 0.59 (MPM) and 0.69 (H&E) indicating a substantial level of agreement between the 38 raters.

Discussion

This is the first online survey among a group of international pediatric pathologists to evaluate the potential of MPM versus conventional HP to diagnose normal pediatric tissues, neuroblastoma and rhabdomyosarcoma. The study was conducted as an international online survey using a commercially available survey platform which proved very suitable for this type of study because a worldwide participation was recruitable and constructing the survey was relatively simple. The quality of the uploaded images was rated to be excellent by study participants, reflected by the fact that they almost reached 100% correct diagnostic accuracy when presented with the conventional HP images, arguably representing the gold standard for pathologists. The mean time invested by each participating pathologist was under 30 mins. Likewise, assessment of both the MPM conventional HP pictures showed good level of agreement between the raters.

The optimal image generation using MPM technology required some experience and routine, in particular with regard to the laser parameters, such as optimal gain, transmission and wavelength. In prior studies, we established the optimal laser settings for the desired tissue examinations by trial and error.

The study results showed that currently, and without prior training to the novel method, pediatric pathologists are more accurate in making a diagnosis on conventional HP, but that they are able to discern certain key features on MPM as well. While MPM lacked sensitivity for diagnosing the tumors, it was quite specific (when pathologists did indeed make the diagnoses, they were universally correct). This goes along with some published studies, which described MPM as a very specific and accurate method in gastric and bladder cancer evaluation.[6,16] Nevertheless, this study was not designed to highly prove the issue of diagnostic sensitivity and specificity. It gives a good hint, which needs to be analyzed by a much larger number of tumor types and samples.The difference in diagnostic accuracy may be due to the fact that pediatric pathologists are simply naive in interpreting MPM images, while it is their daily work to make diagnoses from conventional HP. This study may have assessed the situation before the

Table 3 Evaluation of specific parameters of the individual tissues (MPM versus conventional HP (H&E); mean grading system (0 [not visible], 1 [suggested without details], 2 [recognizable without further details], 3 [recognizable including all details]). Significantly better rating marked in bold and italics

	MPM	H&E	*P*
Liver [mean, 95% CI:]			
Sinusoid	1.50 [1.25–1.75]	**2.84 [2.72–2.96]**	<0.001
Hepatocytes	1.68 [1.45–1.91]	**2.89 [2.79–3.00]**	<0.001
Biliary tract	1.87 [1.65–2.09]	**2.79 [2.65–2.93]**	<0.001
Glisson´s triad	2.29 [2.03–2.54]	**2.82 [2.69–2.94]**	<0.001
Cell nuclei	0.97 [0.72–1.22]	**2.87 [2.76–2.98]**	<0.001
Lung [mean, 95% CI:]			
Bronchiolus	2.34 [2.12–2.56]	2.71 [2.54–2.88]	n.s.
Vessel branch of the pulmonal artery	2.11 [1.87–2.34]	**2.76 [2.60–2.92]**	<0.001
Alveoli	2.18 [1.94–2.42]	**2.79 [2.60–2.98]**	<0.001
Alveolar macrophages	1.03 [0.68–1.35]	**1.92 [1.62–2.22]**	<0.001
Cell nuclei	0.76 [0.55–0.97]	**2.42 [2.21–2.63]**	<0.001
Heart [mean, 95% CI]			
Connective tissue	2.42 [2.18–2.66]	2.26 [2.03–2.50]	n.s.
Disci intercalares	**2.55 [2.33–2.78]**	1.45 [1.16–1.73]	<0.001
Capillary vessels	1.47 [1.16–1.79]	1.79 [1.46–2.12]	n.s.
Cell nuclei	0.68 [0.45–0.91]	**2.71 [2.54–2.88]**	<0.001
Kidney [mean, 95% CI]			
Glomerulus	2.08 [1.82–2.34]	**2.82 [2.67–2.97]**	<0.001
Afferent/efferent vessel	1.34 [1.03–1.65]	**1.89 [1.58–2.21]**	0.002
Collection tubuli	1.97 [1.70–2.24]	**2.82 [2.69–2.94]**	<0.001
Cell nuclei	1.05 [0.81–1.29]	**2.74 [2.59–2.88]**	<0.001
Adrenal gland [mean, 95 % CI]			
Capsule	2.79 [2.63–2.95]	2.76 [2.60–2.92]	n.s.
Zona glomerulosa	2.11 [1.80–2.41]	**2.58 [2.40–2.76]**	<0.001
Zona fasciculata	1.95 [1.63–2.26]	**2.47 [2.28–2.67]**	<0.001
Zona reticularis	1.79 [1.48–2.10]	**2.34 [2.07–2.61]**	<0.001
Adrenal medulla	1.18 [0.86–1.51]	**1.79 [1.39–2.19]**	<0.001
Cell nuclei	0.84 [0.65–1.04]	**2.53 [2.31–2.74]**	<0.001
Testicle [mean, 95% CI]			
Tunica albuginea testis	2.76 [2.57–2.96]	2.79 [2.63–2.95]	n.s.
Tubuli seminiferi contorti	2.45 [2.21–2.69]	2.63 [2.39–2.87]	n.s.
Septum testis	**2.34 [2.07–2.61]**	1.76 [1.42–2.10]	0.001
Lamina limitans	2.08 [1.81–2.35]	1.84 [1.55–2.13]	n.s.
Blood vessels	2.42 [2.17–2.67]	2.29 [2.13–2.65]	n.s.
Cell nuclei	0.95 [0.71–1.19]	**2.29 [2.13–2.65]**	<0.001
Neuroblastoma [mean, 95% CI]			
Neuroblasts with small round nuclei	0.79 [0.56–1.01]	**2.42 [2.21–2.63]**	<0.001
Nuclei with stippled chromatin	0.45 [0.21–0.69]	**1.87 [1.56–2.18]**	<0.001
Indistinct cell borders	0.79 [0.52–1.06]	**1.97 [1.68–2.26]**	<0.001
Ganglion cells prominent nucleoli	0.53 [0.25–0.80]	**1.74 [1.36–2.11]**	<0.001
Stroma with tumor vessels	1.68 [1.34–2.03]	2.05 [1.78–2.33]	n.s.
Atypical cells	0.47 [0.25–0.70]	**2.05 [1.79–2.32]**	<0.001
Rhabdomyosarcoma [mean, 95% CI]			
Rhabdomyoblasts	1.50 [1.22–1.78]	**2.79 [2.65–2.92]**	<0.001

(*Continued*)

Table 3 (Continued).

	MPM	H&E	*P*
Indistinct cell borders	1.16 [0.86–1.46]	**2.16 [1.83–2.49]**	<0.001
Atypical cells	1.29 [0.94–1.64]	**2.53 [2.23–2.82]**	<0.001
Myxoid stroma with vessels	0.92 [0.62–1.22]	**1.97 [1.65–2.29]**	<0.001
Cell nuclei	0.74 [0.46–1.01]	**2.39 [2.18–2.60]**	<0.001

Note: Statistically significant values are shown in bold
Abbreviations: MPM, multiphoton microscopy; H&E, hematoxylin-eosin; n.s., non-significant.

Table 4 Selected evaluation of cell nuclei (MPM versus conventional HP (H&E); mean grading system (0 [not visible], 1 [suggested without details], 2 [recognizable without further details], 3 [recognizable including all details]). Significantly better rating marked in bold and italics

	MPM	H&E	*P*
Cell nuclei [mean, 95-%-CI]			
Liver	0.97 [0.73–1.22]	**2.87 [2.76–2.98]**	<0.001
Lung	0.76 [0.56–0.97]	**2.42 [2.21–2.63]**	<0.001
Heart	0.68 [0.45–0.92]	**2.71 [2.54–2.88]**	<0.001
Kidney	1.05 [0.81–1.29]	**2.74 [2.59–2.88]**	<0.001
Adrenal gland	0.84 [0.65–1.04]	**2.53 [2.31–2.74]**	<0.001
Testicle	0.95 [0.71–1.19]	**2.30 [2.14–2.65]**	<0.001
Neuroblastoma	0.45 [0.21–0.69]	**1.87 [1.56–2.18]**	<0.001
Rhabdomyosarcoma	0.74 [0.47–1.01]	**2.40 [2.19–2.61]**	<0.001

Note: Bold values indicate H&E was statistically significantly superior to MPM for the evaluation of cell nuclei in all normal tissues and tumor tissues.
Abbreviation: n.s., non-significant; MPM, multiphoton microscopy; H&E, hematoxylin-eosin.

learning curve. Similar findings have been published by Neumann et al for confocal laser endomicroscopy (CLE) in IBD.[17] In this study, significant improvement in CLE performance over time was described, including decreased confocal imaging time, successful CLE diagnosis and decline in procedural time. Strikingly, these diagnostic quality parameters improved significantly already after the initial three cases.

In order to take full advantage of the capabilities of MPM, we recognized in this study that MPM seems to be very useful for the recognition of "protein-rich" structures such as the disci intercalares. It may be less applicable to assess the cell nuclei, regardless of tissue types. Knowing these advantages and drawbacks may allow for the purposeful application for specific diagnostic indications. These findings may guide the standardization of imaging protocols in the future,[18,19] but fully answering this question has to be addressed specifically across multiple tissue and tumor types using a more reliable definition of "protein rich".

In particular, the high differentiability of connective tissue-containing structures may be suitable for intraoperative demarcation of "protein-rich" tumors like sarcomas in the future. This would underline the usefulness of a development of an intraoperatively usable MPM, especially to determine resection margins more clearly. However, there are no published studies on the intraoperative use of MPM to date and any thoughts about intraoperative utility remain highly speculative. In an unpublished study we estimated the distinction between tumor tissue and normal tissue in adrenal neuroblastoma and nephroblastoma, and per our experience and the experience of our local pathology team, this was possible with good quality. Nevertheless, a large amount of additional studies have to be conducted on resected tissue that is representative of the clinical situation to conclude good answers. Also, the MPM hardware would need to be adapted to the clinical situation. Smaller, benchtop MPM devices would be necessary to image resected tissue inside the OR. Alternatively, another useful development would be a sterilizable device that can image the tissues directly and real-time in the patient, in vivo. Initial experimental studies are heading in this direction.[11]

Table 5 Selected pre-determined characteristics assessed in the evaluation of connective tissue-containing structures

Organ	Item
Liver	Biliary tract Glisson´s triad Sinusoids
Lung	Bronchiolus Vessel branch of the pulmonary artery
Heart	Connective tissue Disci intercalares Capillary vessels
Kidney	Glomerulus Collection tubuli
Testicle	Tunica albuginea Tubuli seminiferi contorti Septum testis Blood vessels Lamina limitans
Neuroblastoma Adrenal gland	Stroma with tumor vessels
Rhabdomyosarcoma Urinary bladder	Myxoid stroma with vessels

Besides cancer, Hirschsprung disease may be another interesting application for in vivo MPM imaging to determine the transition zone between ganglionated and aganglionated bowel.[20]

Also, dermatologist developed some mobile MPM devices that explicitly target the evaluation of skin lesions and skin tumors.[21,22] The field of dermatology is very interesting for MPM, as there are already good scientific papers published on skin tumors and as the devices look externally at the patient, which makes it more easy to use MPM in clinical praxis. The futural development of such devices for surgery seems desirable. Dimitrow et al for instance screened melanocytic skin lesions from 83 human patients for the pigmented skin melanoma with TPM.[23] Four imaging features, such as architectural disarray of epidermis, poorly defined keratinocyte cell borders, presence of dendritic cells and presence of pleomorphic cells, were identified from large intercellular distance and ascending melanocytes as indicator for diagnosis of malignant melanoma with 85% and 97% accuracy for in vivo and ex vivo examination, respectively. MPM demonstrated clearly the ability to distinguish human skin biopsies with skin cancers. Incidentally, MPM is shown to be very tissue compatible and has low side effects. The used excitation wavelengths (typically >700 nm) and the limited laser power reduce the potential risk of cell and tissue damage to a minimum, which makes it, in our opinion, also compatible in children.[24]

There are several limitations to our study. One of them is the relatively low participation rate, which could result in a bias toward those pathologists interested in new technology and new techniques. Also, there was no prior training in MPM and, therefore, pathologists simply lacked experience in evaluating MPM images. Finally, there are no standardized MPM imaging protocol available, as any reference data of pediatric normal and tumor tissue were missing initially. These have to be developed with more experience in imaging pediatric tissues and tumors in the future.

Nevertheless, our study for the first time introduces a new, interesting concept of using a commercially available online survey tool to evaluate a new imaging technique. Without a doubt, the MPM imaging needs more tuning, the standardization of imaging protocols, and it would be useful to give some basic training on how to interpret the MPM images, including the concept of highlighting collagen fibers detected by second harmonic generation and presenting them in red, as well as presenting cellular proteinaceous components detected by autofluorescence in green. Prior training of the raters may also further increase the IRR.[25]

Another interesting aspect for MPM as a novel imaging technique would be the assessment using artificial intelligence. This may objectify the assessment and make it less user-dependent.[26]

Conclusion

To our knowledge, this is the first application of an online survey tool among a group of international pediatric pathologists to evaluate the potential of MPM versus conventional HP to diagnose benign and neoplastic tissues in childhood. We thereby have documented the potential of MPM for diagnosing normal and cancerous tissue along with pitfalls that need to be addressed in the future. AT this time, MPM is not ready to compete with the gold standard methods in pathology evaluation, but may be useful as an adjunct, for instance for questions regarding protein-rich structures. As a real-time method that theoretically can be used in vivo, MPM may bridge the gap between surgeon and pathologist in the future,

bringing pathologists to the patient's bedside and offering surgeons an instant microscopic characterization of the tissue of concern. "Interventional pathologists" could work side-by-side with the surgeon in the operating room, obviating the need for tissue transport, frozen section, and conveying the resulting information by telephone or through third persons. The described workflow may have the potential of significantly shortening operative times and increasing the rate of complete (R0) tumor resections.

As a next step, we are planning to assess the learning curve of pathologists with MPM and to see if with increasing experience, the diagnostic accuracy approaches that of conventional HP using H&E slides.

In our experience, every individual tissue may require its own specific imaging protocol. We therefore are constantly optimizing our parameters using different wavelengths, filter combinations and fields-of-view. Further research in this regard is definitively warranted.

Acknowledgments

This work was supported by Sterntaler e.V. Mainz and the Else Kröner-Fresenius-Foundation, Germany. This paper was presented in part at the 135th Congress of the German Society of Surgery,[27] and is part of a doctoral thesis by PS[28] and a PhD thesis by JG.[29]

Disclosure

The authors report no conflicts of interest in this work.

References

1. Coffin CM, Spilker K, Zhou H, et al. Frozen section diagnosis in pediatric surgical pathology: a decade's experience in a children's hospital. *Arch Pathol Lab Med*. 2005;129:1619–1625.
2. Carrasco A Jr, Caldwell BT, Cost CR, et al. Reliability of intraoperative frozen section for the diagnosis of renal tumors suspicious for malignancy in children and adolescents. *Pediatr Blood Cancer*. 2017;64(8):e26458. doi:10.1002/pbc.v64.8
3. Dall'igna P, d'Amore ES, Cecchetto G, et al. Intraoperative examination (IOE) in pediatric extracranial tumors. *Pediatr Blood Cancer*. 2010;54:388–393. doi:10.1002/pbc.22309
4. Jain M, Robinson BD, Wu B, Khani F, Mukherjee S. Exploring multiphoton microscopy as a novel tool to differentiate chromophobe renal cell carcinoma from oncocytoma in fixed tissue sections. *Arch Pathol Lab Med*. 2018;142(3):383–390. doi:10.5858/arpa.2017-0056-OA
5. Jain M, Robinson BD, Aggarwal A, Shevchuk MM, Scherr DS, Mukherjee S. Multiphoton microscopy for rapid histopathological evaluation of kidney tumours. *BJU Int*. 2016;118(1):118–126. doi:10.1111/bju.13377
6. Jain M, Robinson BD, Shevchuk MM, et al. Multiphoton microscopy: a potential intraoperative tool for the detection of carcinoma in situ in human bladder. *Arch Pathol Lab Med*. 2015;139(6):796–804. doi:10.5858/arpa.2014-0076-OA
7. Jain M, Narula N, Aggarwal A, et al. Multiphoton microscopy: a potential "optical biopsy" tool for real-time evaluation of lung tumors without the need for exogenous contrast agents. *Arch Pathol Lab Med*. 2014;138(8):1037–1047. doi:10.5858/arpa.2013-0122-OA
8. Durand M, Jain M, Aggarwal A, et al. Real-time in vivo periprostatic nerve tracking using multiphoton microscopy in a rat survival surgery model: a promising pre-clinical study for enhanced nerve-sparing surgery. *BJU Int*. 2015;116(3):478–486. doi:10.1111/bju.12903
9. Liu G, Kieu IK, Wise FW, Chen Z. Multiphoton microscopy system with a compact fiber-based femtosecond-pulse laser and handheld probe. *J Biophot*. 2011;4:34–39. doi:10.1002/jbio.201000049
10. Helmchen F, Denk W, Kerr JN. Miniaturization of two-photon microscopy for imaging in freely moving animals. *Cold Spring Harb Protoc*. 2013;10:904–913.
11. Duan X, Li H, Qiu Z, et al. MEMS-based multiphoton endomicroscope for repetitive imaging of mouse colon. *Biomed Opt Express*. 2015;6(8):3074–3083. doi:10.1364/BOE.6.003074
12. Muensterer OM, Waldron S, Boo YJ, et al. Multiphoton microscopy: a novel diagnostic method for solid tumors in a prospective pediatric oncologic cohort, an experimental study. *Int J Surg*. 2017;48:128–133. doi:10.1016/j.ijsu.2017.10.038
13. Cohen JF, Korevaar DA, Altman DG, et al. STARD 2015 guidelines for reporting diagnostic accuracy studies: explanation and elaboration. *BMJ Open*. 2016;6(11):e012799. doi:10.1136/bmjopen-2016-012799
14. Bossuyt PM, Reitsma JB, Bruns DE, et al. STARD 2015: an updated list of essential items for reporting diagnostic accuracy studies. *BMJ*. 2015;351:h5527. doi:10.1136/bmj.h6432
15. Randolph JJ. Free-marginal multirater kappa (multirater K[free]): an alternative to fleiss' fixed-marginal multirater kappa. *Online Submiss*; 2005. Available from: http://eric.ed.gov/?id=ED490661 (Availability checked on November 26, 2018).
16. Yan J, Zheng Y, Zheng X, et al. Real-time optical diagnosis of gastric cancer with serosal invasion using multiphoton imaging. *Sci Rep*. 2016;6:31004. doi:10.1038/srep31004
17. Neumann H, Vieth M, Atreya R, et al. Prospective evaluation of the learning curve of confocal laser endomicroscopy in patients with IBD. *Histol Histopathol*. 2011;26(7):867–872. doi:10.14670/HH-26.867
18. Koenig K, Tanke HJ, Schneckenburger H. Laser microscopy. *Proc SPIE*. 2000;4164:18–27.
19. König K, Schenke-Layland K, Riemann I, et al. Multiphoton autofluorescence imaging of intratissue elastic fibers. *Biomaterials*. 2005;26(5):495–500. doi:10.1016/j.biomaterials.2004.02.059
20. Aggarwal A, Jain M, Frykman PK, Xu C, Mukherjee S, Muensterer OJ. Multiphoton microscopy to identify and characterize the transition zone in a mouse model of Hirschsprung disease. *J Pediatr Surg*. 2013;48:1288–1293. doi:10.1016/j.jpedsurg.2013.03.025
21. Balu M, Zachary CB, Harris RM, et al. In vivo multiphoton microscopy of basal cell carcinoma. *JAMA Dermatol*. 2015;151(10):1068–1074. doi:10.1001/jamadermatol.2015.0453
22. Pouli D, Balu M, Alonzo CA, et al. Imaging mitochondrial dynamics in human skin reveals depth-dependent hypoxia and malignant potential for diagnosis. *Sci Transl Med*. 2016;8(367):367ra169. doi:10.1126/scitranslmed.aaf0746
23. Dimitrow E, Ziemer M, Koehler MJ, et al. Sensitivity and specificity of multiphoton laser tomography for in vivo and ex vivo diagnosis of malignant melanoma. *J Invest Dermatol*. 2009;129(7):1752–1758. doi:10.1038/jid.2008.439
24. Zieger M, Springer S, Koehler MJ, Kaatz M. Multiphoton tomography. *Hautarzt*. 2015;66:511–521. doi:10.1007/s00105-015-3626-9
25. McHugh ML. Interrater reliability: the kappa statistic. *Biochem Medica*. 2012;22:276–282. doi:10.11613/BM.2012.031
26. Huttunen MJ, Hassan A, McCloskey CW, et al. Automated classification of multiphoton microscopy images of ovarian tissue using deep learning. *J Biomed Opt*. 2018;23(6):1–7. doi:10.1117/1.JBO.23.6.066002

27. Simon F, Schreiber P, Goedeke J, Seidmann L, Muensterer O Multiphoton microscopy: *Establishing a new diagnostic method to evaluate pediatric tissues and tumors.* Paper presented in part at the 135th Congress of the German Society of Surgery, Berlin, April 20, 2018
28. Schreiber P. *Multiphoton microscopy in the diagnostic assessment of different pediatric solid tissues in comparison to conventional histopathology* [doctoral thesis]. Mainz: Johannes Gutenberg University; 2019.
29. Goedeke J. *Innovative new ways in diagnosis and treatment of various malignant extracranial solid tumors in childhood and adolescence* [PhD thesis]. Mainz: Johannes Gutenberg University; 2019.

Video abstract

Point your SmartPhone at the code above. If you have a QR code reader the video abstract will appear. Or use: https://youtu.be/gvwMDx3dyN0